Catalysis Letters (2021) 151:1038–1048
https://doi.org/10.1007/s10562-020-03364-z

Catalytic Conversion of Chloromethane to Olefins and Aromatics Over Zeolite Catalysts

Di Zhu[1] · Zi Wang[2] · Fei Meng[2] · Baofeng Zhao[1] · Swarom Kanitkar[3] · Yongchun Tang[2]

Received: 5 June 2020 / Accepted: 21 August 2020 / Published online: 7 September 2020

Abstract

We report the tunable conversion of chloromethane to olefins and aromatics using different metal-promoted zeolites as catalysts. Despite SAPO-34 was industrially used as catalysts for methanol to olefins reaction (MTO), the SAPO-34 based zeolites exhibited low activity and short lifetime when using chloromethane as the feed. Higher chloromethane conversion and longer catalyst lifetime were found on H-ZSM-5. The activity and product distribution can be improved by optimizing the reaction temperature and space velocity. Impregnating the H-ZSM-5 zeolite with 1 wt% and 5 wt% metal oxide as promoters significantly enhanced the conversion efficiency and altered the product distribution. The highest aromatics selectivity (38%) was obtained on the H-ZSM-5 zeolite promoted by 5 wt% Ni, whereas on 5 wt% Mg and 5 wt% Mn promoted H-ZSM-5, the aromatics selectivity is merely 5%. Therefore, different modified H-ZSM-5 could be used to convert chloromethane to either aromatics or olefin-heavy products. It was found that the aromatics yield is strongly correlated to the acidity of the H-ZSM-5 zeolite.

Di Zhu and Zi Wang have contributed equally to this study.

Electronic supplementary material The online version of this article (https://doi.org/10.1007/s10562-020-03364-z) contains supplementary material, which is available to authorized users.

✉ Zi Wang
zi.wang@peeri.org

[1] Key Laboratory for Biomass Gasification Technology of Shandong Province, Energy Research Institute, Qilu University of Technology (Shandong Academy of Sciences), Jinan 250014, China

[2] Power Environmental Energy Research Institute, 738 Arrow Grand Circle, Covina, CA 91722, USA

[3] Department of Chemical Engineering, Louisiana State University, Baton Rouge, LA 70803, USA

Graphic Abstract

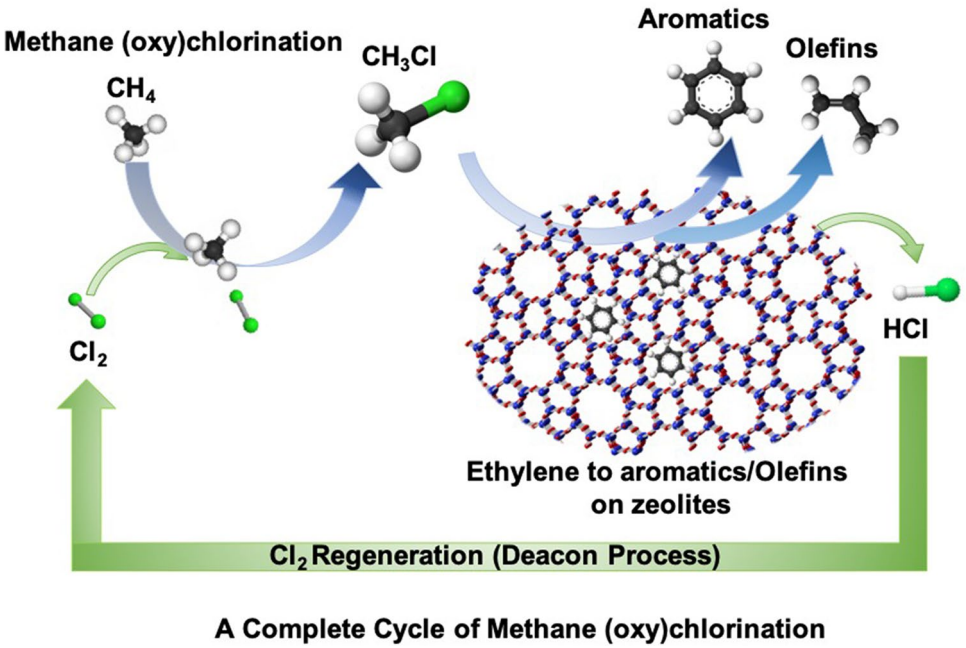

Keywords Chloromethane · H-ZSM-5 · SAPO-34 · Olefins · Aromatics

1 Introduction

With the abundant reserves and desirable carbon-hydrogen ratio, methane (CH_4), the major component of shale gas, is a promising starting material to synthesize important industrial chemical intermediates such as light olefins(C_2–C_4) and aromatics (benzene, toluene and xylene). Currently the only industrial approach to convert methane is through the syngas route, which demand high operating temperature and capital cost. On the other hand, the direct methane conversion processes are potentially more cost-effective and environmentally friendly than the syngas route. These methods include pyrolysis [1, 2], oxidative coupling of methane [3], superacid catalysis [4, 5], halogenation [6, 7], etc. Among all these processes, the conversion of methane to chloromethane (CH_3Cl) has been drawing increasing attention since the temperature requirement is much less aggressive comparing to the traditional syngas approaches. In this route, methane is converted to chloromethane by reacting with chlorine using oxychlorination [7–9] or light/thermal initiation [10–12]. The reaction temperature for the oxychlorination process is between 350 and 450 °C; and for light initiation, methane chlorination can be conducted even at room temperature.

The main product of methane halogenation, i.e. chloromethane (CH_3Cl), has limited direct applications [13, 14]. Nevertheless, CH_3Cl can serve as a versatile chemical intermediates to form ethylene, propylene, and aromatics (Eq. 1). Moreover, chlorine can be regenerated from the HCl byproduct via the Deacon process (Eq. 2), and can eventually be recycled for methane chlorination.

$$n CH_3Cl \rightarrow C_nH_{2n} + nHCl \quad (1)$$

$$2HCl + \frac{1}{2}O_2 \rightarrow H_2O + Cl_2 \quad (2)$$

The catalysts used in chloromethane conversion are typically bifunctional acid–base catalysts and several shape-selective microporous zeolites [15–19]. Su et al. [18, 20–24] studied the chloromethane conversion over SAPO-34, which has been proved to be the most excellent MTO catalyst [25]. A conversion of 70% was reached at 500 °C, with the C_2 products dominating the product distribution (approximately 40% $C_{2=}$, excluding coke). Other zeolites, such as MCM-22, ZSM-11 or SAPO-5 were also tested for chloromethane conversion. However, the performances of these zeolites are not satisfying due to low chloromethane conversion, low olefin selectivity, high coking rate, or short catalyst lifetime.

Here we report a series of metal-promoted H-ZSM-5 zeolites exhibiting superior performance on the conversion of chloromethane to olefins or aromatics. The catalysts exhibited above 90% CH_3Cl conversion over 3 h of time on stream, and product selectivity towards 90% olefin or 40% aromatics, depending on the choice of the promoters and

reaction conditions. Various types of zeolite in combination with different metal loadings were investigated and optimized for the chloromethane conversion. The reaction conditions, including temperature, space velocity, catalyst regeneration procedure, etc. were also optimized to improve the catalyst selectivity and extend the lifetime of the catalyst.

2 Experimental

2.1 Catalyst Preparation

NH_4-ZSM-5(Alfa Aesar, Si:Al = 30, specific surface area = 400 m^2/g) and SAPO-34 (ACS Materials LLC, specific surface area ≥ 550 m^2/g) were used in the study. H-ZSM-5 was obtained by calcining NH_4-ZSM-5 at 550 °C in static air for 3 h. For metal-impregnated catalysts, $Ni(NO_3)_2{\cdot}6H_2O$, $Mg(NO_3)_2{\cdot}6H_2O$, and $Mn(NO_3)_2{\cdot}xH_2O$ were used as metal precursors. To obtain different wt% of metal in H-ZSM-5 zeolite, a desired amount of Ni, Mg or Mn nitrates were dissolved in water, and H-ZSM-5 was slowly added into the solution under vigorous stirring. The slurry was stirred for 12 h, followed by heating to 80 °C to evaporate the water. The sample was then dried at 120 °C and calcined at 550 °C for 3 h. All the catalysts were crushed and sieved to obtain 50 mesh particles prior to catalyst testing.

2.2 Catalyst Testing

A continuous-flow fixed-bed reactor with an 8 mm i.d. quartz tube was used for CH_3Cl to olefins and aromatics reaction. The reactor was operated at different temperatures ranging from 325 to 475 °C, and the space velocity for CH_3Cl varied from 1.3 to 3.3 h^{-1}. In each test, a mixed flow of $CH_3Cl:N_2 = 1:3$ was flowed into the reactor, and the weight of catalyst was adjusted to yield different space velocity. The effluent gas was analyzed by an Agilent 7890 gas chromatograph (GC) that is equipped with a flame ionization detector (FID) and a thermal conductivity detector (TCD). The tubing after the reactor was heated to 180 °C to eliminate condensation of the products. After each run, the quartz tube with the spent catalyst inside was detached from the reactor and the total weight of the quartz tube + catalyst was measured, which is named as w1. Then the catalyst was calcined at 800 °C, and the total weight was measured again, named as w2. The weight of coke accumulated during the reaction is the difference of w1 and w2. The mass balance in all experiments were 95–100% based on carbon.

2.3 Ammonia Temperature-programmed Desorption (NH_3-TPD)

NH_3-TPD was carried out on an Altamira-300 reactor system (Altamira Instruments Inc.) in conjunction with an Ametek LC-D Mass Spectrometer. In a typical test, 50 mg of catalyst was loaded into a U-shape quartz tube reactor. The catalyst was firstly heated at 120 °C under He flow for 30 min, then cooled down to 50 °C. Ammonia adsorption was performed at 50 °C by flowing 40 sccm of NH_3 through the reactor for 1 h. After the adsorption, 25 sccm of He was flowed for 40 min to remove residual ammonia. The reactor was then heated to 600 °C with a ramp rate of 10 °C/min to desorb the chemisorbed ammonia. Mass spectrometer was turned on during the ramping step to detect the desorbed ammonia in the effluent gas.

2.4 BET Surface Area

Specific surface areas of the catalysts were examined by a 3H-2000PS1 (BeiShiDe Instrument Technology) according to the Brunauer–Emmett–Teller (BET) method. The pressure range for N_2 adsorption/desorption is between 0.04 and 0.32. The micropore volume were analyzed using the T-plot method.

2.5 X-ray Diffraction

XRD analysis was performed on a PANalytical Empyrean XRD Diffractometer with Cu Kα radiation in the 5°–50° 2θ range. Step width and scanning speed were set at 0.02° and 2°/min, respectively.

3 Results and discussion

3.1 Chloromethane Conversion on Unmodified Zeolites

The chloromethane conversion reaction and the MTO/MTA reaction share immense similarity since the CH_3Cl and CH_3OH are structurally alike. Thus, similar reaction conditions and catalysts for MTO/MTA were often adapted to catalyze the chloromethane conversion. In this work, we also started with plain, untreated zeolites, including H-ZSM-5 and SAPO-34, to lay down the groundwork and find out the ideal reaction conditions for chloromethane conversion. The performance of the unprompted H-ZSM-5 and SAPO-34 at different reaction temperatures are summarized in Table 1. Coke selectivity is not included in this section since the temperature was continuously changing during the analysis. For H-ZSM-5 zeolite, the temperature ramped from 375 to 525 °C with a 50 °C step size, and the reaction data was

Table 1 Chloromethane conversion over H-ZSM-5 and SAPO-34 at different temperatures

Catalyst	Temperature °C	Product selectivity %									CH_3Cl conversion%
		CH_4	Ethane	C2 =	C3 =	C4 =	C5 =	Benzene	Toluene	C8	C9	
H-ZSM-5	375.00	0	0.98	13.72	32.72	46.09	6.49	N.D	N.D	N.D	N.D	27.11
	425.00	0	1.25	14.99	30.96	28.24	6.27	2.13	0.00	5.00	11.16	63.22
	475.00	2.74	1.52	21.25	30.24	19.08	3.39	1.73	3.46	5.34	11.24	80.91
	525.00	10.99	1.84	23.95	21.81	9.48	1.80	1.63	6.21	10.66	11.63	83.22
SAPO-34	325.00	0	0.64	18.49	60.13	7.13	13.61	N.D	N.D	N.D	N.D	23.73
	375.00	0	0.85	25.46	56.93	7.08	9.68	N.D	N.D	N.D	N.D	34.60
	425.00	0	1.58	44.27	46.58	3.44	4.13	N.D	N.D	N.D	N.D	53.49
	475.00	0	2.23	51.32	38.42	3.85	4.18	N.D	N.D	N.D	N.D	84.27

Reaction conditions: WHSV = 2.7 h^{-1}, TOS = 30 min

N.D. not detected

Table 2 Thermodynamic constants and heat of reaction for relevant compounds in chloromethane conversion

Substance	Heat of formation Δh_f^0 (kJ/mol)	Heat of reaction Δh_R^0 (kJ/mol)†
C_2H_4 (g)	52.4	31.6
C_3H_6 (g)	20.41	− 10.79
1-Butene (g)	− 0.4	− 42
Benzene (g)	82.9	20.5
Toluene (g)	50	− 22.8
Styrene (g)	147	63.8
Ethylbenzene (g)	49	− 34.2
p-Xylene (g)	17.9	− 65.3

Source: [29]

†Heat of reaction calculation is described in Equation S3 in supplemental material

recorded after 30 min of reaction at that temperature. On H-ZSM-5, propylene and butylene dominated the product distribution at 375 °C, while ethylene and aromatics (toluene, C8 and C9 components) selectivity increased significantly when the temperature is above 425 °C. A further increase of the reaction temperature yields even higher ethylene and aromatics selectivity, this could be understood from both the thermodynamics and surface reaction perspectives. The Calculation on the reaction enthalpy change of the reactions (Table 2) show that chloromethane to ethylene and styrene reactions are highly endothermic while the reactions for other components are exothermic or less endothermic. Thus, these components are more favorable in the high temperature region. In a surface reaction perspective, Ibáñez et al. [26] claimed that the chloromethane to olefin reaction undergoes the same mechanism with MTO reaction, which is a hydrocarbon pool system with two cycles running simultaneously [27]: Cycle I involves aromatics and ethene formation from the lower methylbenzenes followed by re-methylation, and Cycle II includes C3 + alkenes formation by methylation and cracking. In addition, On H-ZSM-5, Cycle I and II are connected since the higher alkenes formed in the methylation/cracking cycle can be further converted to methylbenzenes via cyclization and hydrogen transfer reactions. The cyclization of alkene is especially favored at high temperatures [27, 28]. Therefore, as the reaction increases, additional higher alkenes are converted into methylbenzenes, which are circulated in Cycle I and generate ethene and aromatics as the final products.

SAPO-34 was also tested following the similar procedure with the temperature ranging from 325 to 475 °C. The catalyst also showed higher ethylene selectivity as the temperature increases. At the end of the experiment, a significant amount of coke were founded on the SAPO-34 catalyst.

Another test was carried out at constant reaction temperature to evaluate the coke selectivity and catalyst deactivation rate. A direct comparison of H-ZSM-5 and SAPO-34 at 425 °C is shown in Table 3. After 60 min of TOS, the main products on H-ZSM-5 were C_2–C_4 olefins, along with an 18.06% total aromatics selectivity and a 2.09%

Table 3 Chloromethane conversion over unmodified zeolites

Catalyst	Product selectivity %									Conversion (%)
	Ethane	C2 =	C3 =	C4 =	C5 =	Benzene	Toluene	C8	C9	Coke	
H-ZSM-5	2.29	18.30	32.15	23.13	4.10	1.80	0.10	4.47	11.60	2.06	73.86
SAPO-34	1.47	41.99	38.00	2.80	3.36	N.D	N.D	N.D	N.D	12.38	74.66

Conditions: 425 °C, WHSV = 2.7 h^{-1}, Time on stream (TOS) = 60 min

coke selectivity. SAPO-34 showed ethylene and propylene as the dominating products, and a substantial amount of coke (12.19%) was detected. In terms of the conversion, the two zeolites had comparable conversions in the first hour of TOS, but SAPO-34 deactivated at a much faster rate than H-ZSM-5, according to Figure S1. Since SAPO-34 showed comparable selectivity results to H-ZSM-5 but more rapid deactivation, chloromethane conversion on SAPO-34 requires either frequent regeneration as is in the MTO process, or further modification of the zeolite with promoters to mitigate coke formation.

The space velocity is also examined in this study as various WHSVs were used for chloromethane conversion before. For example, Su et al. [20, 21, 30] carried out chloromethane conversion at WHSV = 3.17 g_{CH3Cl}/g/h for both H-ZSM-5 and SAPO-34 zeolites, which was inherited from conventional MTO reaction conditions. Lersch and Bandermann [31] performed the reaction at WHSV = 1 g_{CH3Cl}/g/h for their enlarged lab scale aging test on H-ZSM-5 and obtained over 90% of CH_3Cl conversion for their first 20 h of reaction. Figure 1 shows the CH_3Cl conversion and product selectivity for CH_3Cl conversion on H-ZSM-5 zeolite at 425 °C, with different WHSVs ranging from 1.3 to 3.3 g_{CH3Cl}/g/h. The ideal WHSV that maximizes both chloromethane conversion and aromatics selectivity was found at 1.87 g_{CH3Cl}/g/h. At higher WHSVs, the diffusion of reactants becomes the main limitation, causing the decrease of CH3Cl conversion. On the other hand, a lower WHSV yields more coke products (10.5% coke selectivity when WHSV = 1.3 g_{CH3Cl}/g/h), which will reduce the lifetime of the catalysts.

The product distribution of chloromethane conversion over H-ZSM-5 is similar to the results that used methanol as the feed [32–34]. On the other hand, SAPO-34 zeolites deactivate at a much faster rate than that in MTO synthesis under similar reaction conditions, as MTO using SAPO-34 usually retains > 90% conversion for more than 2 h of operation [35–37]. In order to address the deactivation issue, metal oxide promoters were impregnated into the zeolites to evaluate if a higher catalyst reactivity and a lower coke rate could be achieved.

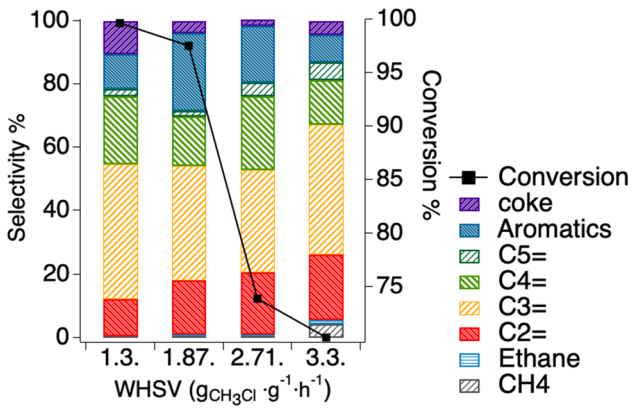

Fig. 1 CH_3Cl conversion and product distribution on H-ZSM-5 at different WHSVs. The black line and ■ mark denote the CH_3Cl conversion rate after 60 min TOS

3.2 Impregnating Metal Oxide Promoters into SAPO-34

Previous studies on SAPO-34 for MTO reaction reported that modifying the zeolite with metal oxides could increase the conversion, inhibit the coke formation, and extend catalyst life time [38–40]. In this study, a variety of metal oxide promoters that were used on SAPO-34 for MTO reaction, including Mg, Mn and Ca, were impregnated into SAPO-34 for chloromethane conversion testing. The weight % of the promoters were set at 1%, and the catalysts were denoted as 1% Me-SAPO-34 (Me=Mg, Mn or Ca). For Mg, 0.5 wt% and 5 wt% of Mg were also impregnated into SAPO-34 zeolites and the samples were denoted as 0.5% Mg-SAPO-34 and 5% Mg-SAPO-34, respectively. The CH_3Cl conversion and product distribution is summarized in Fig. 2, and the change of conversion rate is shown in Figure S3. Metal impregnation seems to have limited effect, if not detrimental, on improving the catalyst activity: Only Mn promoted SAPO-34 showed higher (> 90%) initial CH_3Cl conversion, nevertheless the activity for 1% Mn-SAPO-34 decreases rapidly over the 160 min of time on stream. The deactivation rate was almost identical for blank and metal oxide promoted SAPO-34 zeolites. For the SAPO-34 zeolite impregnated with different Mg loading in SAPO-34, the activity changed from 64% on 0.5% Mg-SAPO-34 to 60% on 1% Mg-SAPO-34, then to 54% on 5% Mg-SAPO-34. According

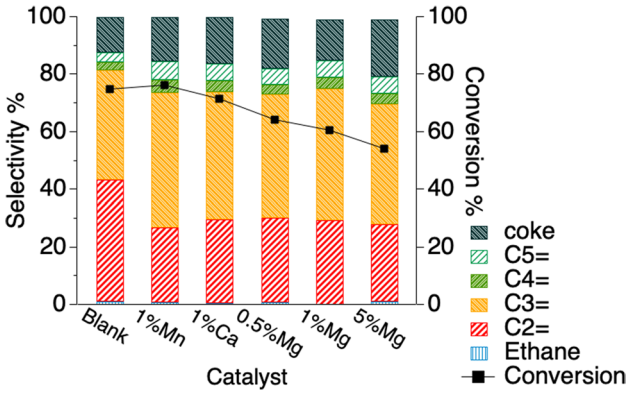

Fig. 2 Catalytic performance for SAPO-34 impregnated with different metal oxides, including the product distribution and CH_3Cl activity after 60 min of reaction. Catalyst impregnated with X wt% of metal Y is denoted as X%YSAPO-34. For instance, 1% MgSAPO-34 is the SAPO-34 sample impregnated with 1 wt% of Mg. Reaction conditions: 400 °C, WHSV = 1.87 h^{-1}

to the BET surface area and pore volume analysis in Table 4, the promoted catalysts have less surface area and smaller micropore volume comparing to the blank SAPO-34 zeolite. As is proven by X-ray Diffraction in Figure S4, impregnating metal nitrate precursors into zeolite materials followed by calcination creates amorphous metal oxide on the zeolite surface. The metal oxide accumulated on the surface and block the pores on SAPO-34, which leads to lower chloromethane conversion while the deactivation rate and product distribution remains the same.

3.3 Impregnating Metal Oxide Promoters into H-ZSM-5

In methanol conversion, H-ZSM-5 were also modified by metal oxide promoters to increase methanol conversion and extend the life time [41, 42]. These metal oxide promoters include several alkaline earth and transition metals, such as zinc, iron, manganese and magnesium, with metal content up to 5% in the catalyst. Furthermore, according to Lersch et al. [31], in chloromethane conversion, the selectivity of aromatics is strongly correlated with the Sanderson electronegativity. Hence the aromatics selectivity should follow the sequence of Mg < Mn < Ni < Cu < Fe < Zn. Unfortunately, we observed that when chloromethane was used as the feed, hydrogen chloride could react with zinc, copper or iron oxides and form volatile metal chlorides which would be leached out of the zeolite. The volatile metal chlorides would crystallize and accumulate in the cooler zones in the reactor system. Therefore, given the proper reaction temperature, the metal element for impregnation needs to be non-volatile in their metal chloride form at the reaction temperature. Based on the characteristics above, Mn, Mg and Ni were selected as metal oxide promoters and impregnated into H-ZSM-5.

Figure 3 summarized the product distribution and the CH_3Cl conversion of the metal-impregnated H-ZSM-5 catalysts. The weight percentage of metallic Mn, Mg and Ni impregnated in the zeolite were controlled at two levels: 1 wt% and 5 wt%. With the optimized temperature and space velocity, all the catalysts showed 85–97% CH_3Cl conversion after 60 min on stream. At 1% metal loading, 1% Mn–H-ZSM-5 and 1% Ni-H-ZSM-5 gave higher C_5 alkene and C_{6+} aromatics selectivity than H-ZSM-5 samples, while on 1% Mg-H-ZSM-5 the aromatics selectivity was suppressed. The electronegativities for divalent Mg, Mn and Ni are 1.32 eV, 1.66 eV and 1.94 eV, respectively [43]. Thus, the Sanderson electronegativity of the metal oxide promoters is highly

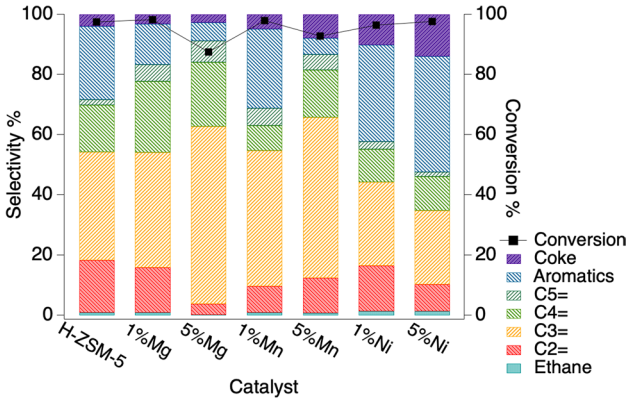

Fig. 3 Change in hydrocarbon distribution for chloromethane conversion over H-ZSM-5 promoted by different metals. Reaction conditions: 425 °C, WHSV = 1.87 h^{-1}, time on stream = 180 min

correlated with the aromatics selectivity. The electronegativity of the metal ions on a solid surface is a rough measure of its Lewis acidity [44, 45], and it also indicates the tendency of an atom to attract electrons [31, 46, 47]. Adding metal cations with higher electronegativity into the zeolites, such as Mn and Ni, will increase the acidity of the zeolite and enhance its ability to attract electrons. As a consequence, the alkene dehydrogenation and cyclization reactions are improved on 1% Mn-H-ZSM-5 and 1% Ni-H-ZSM-5 and more aromatics were obtained.

At 5% metal loading, the aromatics selectivity for 5% Mn-H-ZSM-5 and 5% Mg-H-ZSM-5 were only at 5.5% and 6.5%, respectively. In comparison, on 5% Ni-H-ZSM-5, the total aromatics selectivity was 40%. To sum up, the 5% Mn-H-ZSM-5 and 5% Mg-H-ZSM-5 catalysts have high yield to olefins, while 5% Ni-H-ZSM-5 is more prone to produce aromatics. The trend of aromatics selectivity on the 5% metal-oxide-promoted catalysts does not match the promoters' Sanderson electronegativity of the metallic promoters. The different behavior of aromatics selectivity on 5% Ni vs 5% Mn and 5% Mg promoted zeolites are explained by NH_3-TPD and XRD, which are discussed in the following sections.

3.4 Acidic Properties for Metal Oxide Promoted H-ZSM-5

As shown in previous reports on MTA conversion, the site acidity of H-ZSM-5 can be roughly correlated with the aromatics formation rate [32, 48]. In this study, H-ZSM-5

Table 4 BET surface area and micropore volume parameters of promoted SAPO-34 zeolite

Promoters	1% Mn	1% Ca	0.5% Mg	1% Mg	5% Mg	Blank
BET surface area, m^2/g	454.6	396.5	443.8	430.9	164.3	480.0
Micropore volume, ml/g	0.2371	0.2026	0.2324	0.2192	0.0864	0.245

modified by 5% metal oxide promoters were characterized by NH_3-TPD measurement. Figure 4 shows the NH_3-TPD profiles for the H-ZSM-5 and the 5% metal modified H-ZSM-5 zeolites. The temperatures at the peak maximum for weak, medium and strong adsorption, as well as the NH_3 adsorption amount, are summarized in Table 5. Promoting the zeolites with 5% Mg and 5% Mn had reduced the overall acidity of the zeolite, and eliminated the medium/strong acid sites that desorbs at ~ 400 °C. On 5% Ni H-ZSM-5, the zeolite also showed fewer medium/strong acid sites in the 400 °C ~ 550 °C region, whereas a broad shoulder at 330 °C and a small peak that desorb at 515 °C were detected. The overall acidity on nickel oxide promoted zeolite is slightly higher than un-promoted H-ZSM-5 zeolites. It has been reported that the weak acid sites(150–300°C) are correlated with the Si–OH in the H-ZSM-5 zeolite, whereas the strong acid sites(400–550°C) corresponds to the protonic (Si–OH–Al) and Lewis acid sites [49, 50]. Impregnating 5% Ni into the H-ZSM-5 zeolite caused a significant amount of strong acid sites to transform into the medium strength acid sites. These new acid sites could be ascribed to the interactions between nickel oxide and the protonic or Lewis acid sites in the H-ZSM-5 zeolite. Comparing with blank H-ZSM-5, the 5% Ni-H-ZSM-5 sample contains equal amount of weak acid sites and more medium strength acid sites. The high selectivity to aromatics on 5% Ni-H-ZSM-5 is consistent with the consensus that higher acidity of H-ZSM-5 favors the formation of aromatics [32, 48, 51, 52].

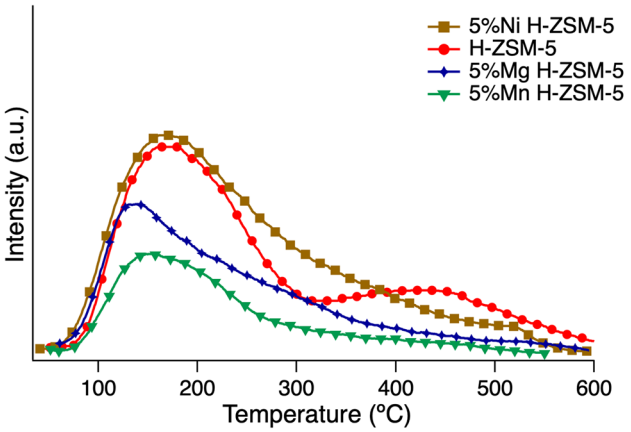

Fig. 4 NH3-TPD pattern of H-ZSM-5 and the metal-promoted H-ZSM-5

As is shown in the NH_3-TPD tests, the H-ZSM-5 zeolite loses acidity when impregnated with 5% Mg and 5% Mn, but gained more acidity when impregnated with 5% Ni. It turns out that the excess coverage of the metallic promoters and the blockage of microchannels could have played a key role in affecting the acidity of the zeolites. A series of XRD were carried out on the blank and 5% metal oxide promoted H-ZSM-5 catalysts. The catalysts were tested once after fresh calcination, and once again after the reaction. In Fig. 5, the catalysts promoted with 5% Mg and 5% Mg showed no extra feature on the XRD pattern than the blank H-ZSM-5 zeolite, indicating that these two promoters are amorphously distributed on the zeolite surface. On the other hand, the freshly calcined 5% Ni-H-ZSM-5 sample showed extra peaks at 37.2° and 43.2°, corresponding to the diffraction peaks for NiO crystallite (PDF#47-1049) [53]. Based on the calculation from the Scherrer equation, the grain size of the NiO crystallite on the 5% Ni-H-ZSM-5 catalyst is around 35 nm. When the H-ZSM-5 zeolite was impregnated with 5% Mg and 5% Mn, a significant amount of amorphous metal oxides accumulated on the catalyst surface, blocking the microchannels and the acid sites, and reducing the surface acidity. On the contrary, for the H-ZSM-5 impregnated with 5% Ni, bulk crystallites were formed on the surface, which means only a fraction of nickel oxide could diffuse into the pores and interact with the acidic sites. By impregnating the zeolite with 5% Ni, the weak acid sites remain unchanged while some of the strong acid sites were affected by nickel oxide promoters and transformed to medium strength acid sites. Therefore, the zeolite acidity could be retained and the catalyst is more selective to aromatics. After 5% Ni-H-ZSM-5 was used for CH_3Cl conversion, the diffraction peaks corresponding to NiO crystallites had reduced in size, which implies that the nickel oxide crystallites may have been leached by the HCl. Reduction in NiO crystallite size also affected the reaction performance. 5% Ni-H-ZSM-5 is not as robust as other metal oxide promoted catalysts in terms of product selectivity. The aromatics selectivity reduced from 46.3 to 27.6% during the 4 h of time on stream (Fig. 6).

Table 5 NH3-TPD results for various metal-promoted H-ZSM-5

Catalyst	T_{max1} (°C)	T_{max2} (°C)	T_{max3} (°C)	NH3 adsorbed (μmol NH_3/g catalyst)
5% Ni-H-ZSM-5	167	330	515	1234.7
H-ZSM-5	162	425	_	1173.8
5% Mn-H-ZSM-5	137	–	_	677.9
5% Mg-H-ZSM-5	150	_	_	876.9

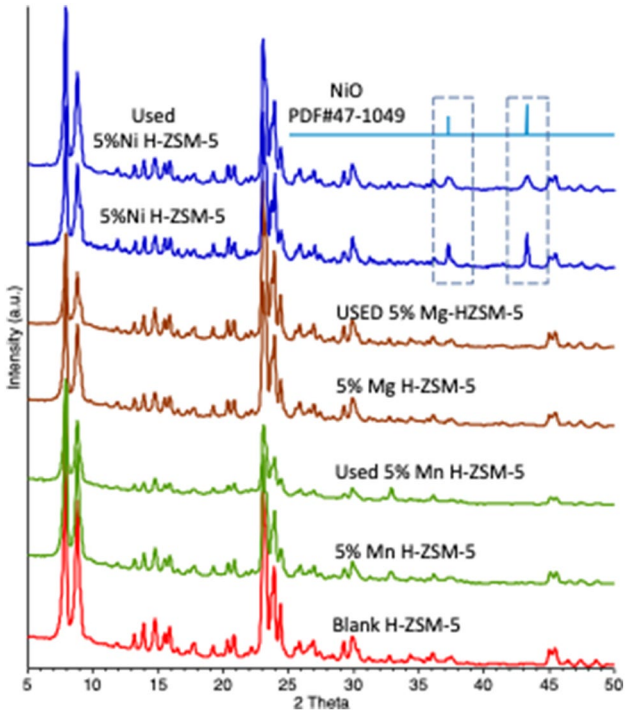

Fig. 5 X-ray Diffraction for calcined and reacted H-ZSM-5 and 5% Me-H-ZSM-5 zeolite

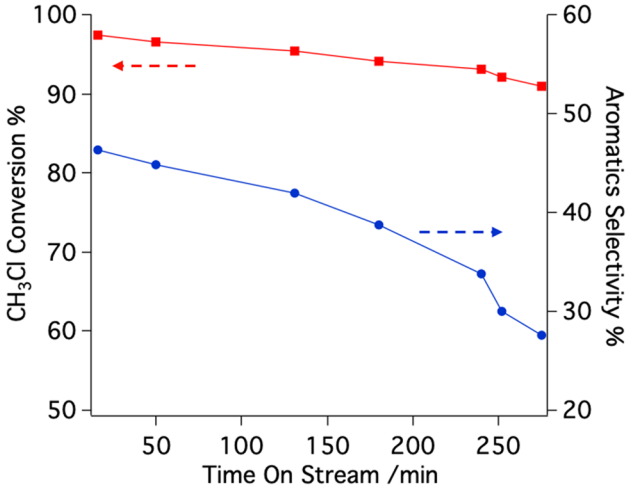

Fig. 6 CH_3Cl Conversion and Aromatics Selectivity of 5% Ni-H-ZSM-5 vs Time On Stream. Reaction Conditions: 425 °C, WHSV = 1.87 h^{-1}

The formation of aromatics and coke is also affected by the Si/Al ratio of the ZSM-5 used in the experiment [27, 54], since the catalytic performance is mostly determined by the number of Brönsted sites in the zeolite. In addition, the anchoring site for metal oxides on H-ZSM-5 may be different when the Si/Al ratio varies [55]. The catalysts tested above were synthesized from the same ZSM-5 zeolite with a Si/Al ratio of 30, which has low silica content and consequently more Brönsted sites. Additional reaction testing were carried out on H-ZSM-5 with a Si/Al ratio of 80 to further study the effect of silica content. As is summarized in Table 6, on blank H-ZSM-5, the zeolite showed lower aromatics selectivity and higher propylene selectivity when the Si to Al ratio was increased from 30:1 to 80:1. Similar behavior was also discovered on samples impregnated with 5% Ni and 5% Mg. In particular, on 5% Mg-H-ZSM-5 with Si/Al = 80, the catalyst displayed < 3% selectivity to aromatics and 65% to propylene. The results have confirmed that the selectivity is concurrently affected by the choice of metal promoters and the Si:Al ratio. A maximized propylene selectivity could be achieved on an Mg promoted H-ZSM-5 with high silica content, and a high aromatics selectivity can be achieved on Ni promoted H-ZSM-5 with low Si:Al ratio.

3.5 Catalyst Regeneration

As is shown above, given the optimized space velocity and temperature, H-ZSM-5 and metal oxide promoted H-ZSM-5 zeolites could retain ~ 90% CH_3Cl conversion over 180 min of reaction. After each run, the catalysts were regenerated by keeping at 800 °C for 1 h under 20% O_2/N_2 flow. A comparison of the reaction performance for 1% Ni, 5% Mg and 5% Ni promoted H-ZSM-5 catalysts and their corresponding regenerated catalysts is shown in Fig. 7. For the regenerated 1% Ni-H-ZSM-5 sample and 5% Ni-H-ZSM-5, which is denoted as "regened 1% Ni" and "regened 5% Ni"in Fig. 7, the chloromethane conversion is identical to the fresh catalyst, except that the regenerated 5% Ni-H-ZSM-5 exhibited less aromatics selectivity. For 5% Mg-H-ZSM-5, the regenerated sample showed slightly higher propylene selectivity and lower C5+ selectivity but the conversion remains the same. In summary, the metal oxide promoted H-ZSM-5 catalysts could be regenerated by air calcination and the catalytic performance is mostly retained after the regeneration.

Table 6 Chloromethane conversion over 30:1 and 80:1 H-ZSM-5

Catalyst	Si: Al	Carbon selectivity							Conversion (%)
		Ethane	C2 =	C3 =	C4 =	C5 =	Aromatics	Coke	
H-ZSM-5	30	0.46	17.80	36.01	15.52	1.85	24.42	3.93	97.47
	80	0.60	16.46	47.85	10.73	4.34	17.06	2.97	79.07
5% Ni-H-ZSM-5	30	0.46	9.78	24.55	11.26	1.50	38.51	13.95	97.65
	80	0.99	15.94	39.49	13.29	2.80	19.59	7.90	84.63
5% Mg-H-ZSM-5	30	0.06	3.66	58.99	21.35	7.16	6.05	2.74	87.50
	80	0.20	7.97	65.44	17.21	5.29	2.63	1.26	89.80

Conditions: 425 °C, WHSV = 1.87 h^{-1}, Time on stream (TOS) = 180 min

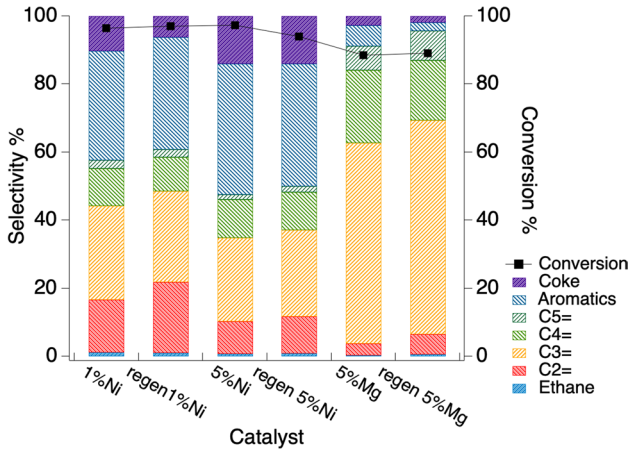

Fig. 7 Catalytic Performance of metal oxide promoted H-ZSM-5 before and after the regeneration. Reaction conditions: 425 °C, WHSV = 1.87 h-1, time on stream = 180 min

4 Conclusion

The chloromethane conversion reaction can be performed on the zeolite catalysts under the conditions similar to the methanol to olefins conversion. However, H-ZSM-5 excels in CH_3Cl activity and catalyst lifetime. In order to maximize the yield to olefins and reduce the coke formation on H-ZSM-5, the reaction should be conducted when the temperature is set at 425 °C and the WHSV is less than 3 h^{-1}. Impregnating the H-ZSM-5 with metal oxide promoters alters the acidity of the zeolites and the aromatics selectivity increases linearly with the acidity of the metal-promoted H-ZSM-5 zeolite. When the H-ZSM-5 is impregnated with 1wt% metal oxide promoters, the aromatics selectivity follows the electronegativity of the metals impregnated. However, when the concentration of the metal oxide reaches 5%, the promoters could accumulate as amorphous phase on the catalyst surface and block the acid sites, thus the aromatics selectivity is significantly lower on the zeolites promoted with 5% Mg and 5% Mn. On the contrary, 5% Ni-H-ZSM-5 showed higher aromatics selectivity than blank H-ZSM-5 since most nickel oxide exhibited as bulk crystallites, thus the overall acidity could be retained. Nickel oxide promoters diffused into the H-ZSM-5 cages helped transform strong acid sites into medium strength acid sites, which also contributed to the formation of aromatics. The aromatics selectivity also decreases when the silica content of ZSM-5 zeolite was increasing. In summary, the product distribution of CH_3Cl reaction on H-ZSM-5 can be adjusted by using different metal oxide promoters. A high aromatics yield was achieved on 5% Ni-H-ZSM-5 while on 5% Mg and 5% Mn promoted H-ZSM-5 the catalyst favors propylene and butylene.

Acknowledgements We are thankful to Louisiana State University, Cain Department of Chemical Engineering on the NH_3-TPD analysis.

References

1. Sun Q, Tang Y, Gavalas GR (2000) Methane pyrolysis in a hot filament reactor. Energy Fuels 14:490–494
2. Fau G, Gascoin N, Gillard P, Steelant J (2013) Methane pyrolysis: literature survey and comparisons of available data for use in numerical simulations. J Anal Appl Pyrol 104:1–9
3. Keller GE, Bhasin MM (1982) Synthesis of ethylene via oxidative coupling of methane: I. Determination of active catalysts. J Catal 73:9–19
4. Crabtree RH (1995) Aspects of methane chemistry. Chem Rev 95:987–1007
5. Kanitkar S, Carter JH, Hutchings GJ, Ding K, Spivey JJ (2018) Low temperature direct conversion of methane using a solid superacid. ChemCatChem 10:5019–5024
6. Olah GA (1987) Electrophilic methane conversion. Acc Chem Res 20:422–428
7. Podkolzin SG, Stangland EE, Jones ME, Peringer E, Lercher JA (2007) Methyl chloride production from methane over lanthanum-based catalysts. J Am Chem Soc 129:2569–2576
8. Lorkovic I, Noy M, Weiss M, Sherman J, McFarland E, Stucky GD, Ford PC (2004) C1 coupling via bromine activation and tandem catalytic condensation and neutralization over CaO/zeolite composites. Chem Commun. https://doi.org/10.1039/B314118G
9. Breed A, Doherty MF, Gadewar S, Grosso P, Lorkovic IM, McFarland EW, Weiss MJ (2005) Natural gas conversion to liquid fuels in a zone reactor. Catal Today 106:301–304

10. Wang B, Albarracín-Suazo S, Pagán-Torres Y, Nikolla E (2017) Advances in methane conversion processes. Catal Today 285:147–158
11. Olah GA, Gupta B, Felberg JD, Ip WM, Husain A, Karpeles R, Lammertsma K, Melhotra AK, Trivedi NJ (1985) Electrophilic reactions at single bonds. 20. Selective monohalogenation of methane over supported acidic or platinum metal catalysts and hydrolysis of methyl halides over.gamma.-alumina-supported metal oxide/hydroxide catalysts. A feasible path for the oxidative conversion of methane into methyl alcohol/dimethyl ether. J Am Chem Soc 107:7097–7105
12. Weissman M, Benson SW (1984) Pyrolysis of methyl chloride, a pathway in the chlorine-catalyzed polymerization of methane. Int J Chem Kinet 16:307–333
13. Holmen A (2009) Direct conversion of methane to fuels and chemicals. Catal Today 142:2–8
14. Van de Walle CG (1993) Wide-band-gap semiconductors, 1st edn. North-Holland, Amsterdam
15. Olah GA, Doggweiler H, Felberg JD, Frohlich S, Grdina MJ, Karpeles R, Keumi T, Inaba S-I, Ip WM, Lammertsma K, Salem G, Tabor D (1984) Onium YLIDE chemistry. 1. Bifunctional acid-base-catalyzed conversion of heterosubstituted methanes into ethylene and derived hydrocarbons. The onium ylide mechanism of the C1 fwdarw. C2 conversion. J Am Chem Soc 106:2143–2149
16. Wei Y, Zhang D, Liu Z, Su B-L (2012) Methyl halide to olefins and gasoline over zeolites and SAPO catalysts: a new route of MTO and MTG. Chin J Catal 33:11–21
17. Taylor CE (2000) Conversion of substituted methanes over ZSM-catalysts. In: Corma A, Melo FV, Mendioroz S, Fierro JLG (eds) Studies in surface science and catalysis. Elsevier, Amsterdam, pp 3633–3638
18. Wei Y, Zhang D, Xu L, Liu Z, Su B-L (2005) New route for light olefins production from chloromethane over HSAPO-34 molecular sieve. Catal Today 106:84–89
19. Svelle S, Aravinthan S, Bjørgen M, Lillerud K-P, Kolboe S, Dahl IM, Olsbye U (2006) The methyl halide to hydrocarbon reaction over H-SAPO-34. J Catal 241:243–254
20. Wei Y, Zhang D, Liu Z, Su B-L (2006) Highly efficient catalytic conversion of chloromethane to light olefins over HSAPO-34 as studied by catalytic testing and in situ FTIR. J Catal 238:46–57
21. Zhang D, Xu L, Du A, Chang F, Su BL, Liu Z (2006) Chloromethane conversion to higher hydrocarbons over zeolites and SAPOs. Catal Lett 109:97–101
22. Wei Y, Zhang D, He Y, Xu L, Yang Y, Su B-L, Liu Z (2007) Catalytic performance of chloromethane transformation for light olefins production over SAPO-34 with different Si content. Catal Lett 114:30–35
23. Wei Y, He Y, Zhang D, Xu L, Meng S, Liu Z, Su B-L (2006) Study of Mn incorporation into SAPO framework: synthesis, characterization and catalysis in chloromethane conversion to light olefins. Microporous Mesoporous Mater 90:188–197
24. Wei Y, Zhang D, Xu L, Chang F, He Y, Meng S, Su B-L, Liu Z (2008) Synthesis, characterization and catalytic performance of metal-incorporated SAPO-34 for chloromethane transformation to light olefins. Catal Today 131:262–269
25. Tian P, Wei Y, Ye M, Liu Z (2015) Methanol to olefins (MTO): from fundamentals to commercialization. ACS Catal 5:1922–1938
26. Ibáñez M, Gamero M, Ruiz-Martínez J, Weckhuysen BM, Aguayo AT, Bilbao J, Castaño P (2016) Simultaneous coking and dealumination of zeolite H-ZSM-5 during the transformation of chloromethane into olefins. Catal Sci Technol 6:296–306
27. Barthos R, Bánsági T, Süli Zakar T, Solymosi F (2007) Aromatization of methanol and methylation of benzene over Mo2C/ZSM-5 catalysts. J Catal 247:368–378
28. Li J, Tong K, Xi Z, Yuan Y, Hu Z, Zhu Z (2016) Highly-efficient conversion of methanol to p-xylene over shape-selective Mg–Zn–Si-HZSM-5 catalyst with fine modification of pore-opening and acidic properties. Catal Sci Technol 6:4802–4813
29. Linstrom PJ, Mallard WG (eds) (2014) NIST chemistry WebBook, NIST standard reference database number 69, National Institute of Standards and Technology, Gaithersburg MD, 20899. https://doi.org/10.18434/T4D303.
30. Zhang D, Wei Y, Xu L, Chang F, Liu Z, Meng S, Su B-L, Liu Z (2008) MgAPSO-34 molecular sieves with various Mg stoichiometries: Synthesis, characterization and catalytic behavior in the direct transformation of chloromethane into light olefins. Microporous Mesoporous Mater 116:684–692
31. Lersch P, Bandermann F (1991) Conversion of chloromethane over metal-exchanged ZSM-5 to higher hydrocarbons. Appl Catal 75:133–152
32. Conte M, Lopez-Sanchez JA, He Q, Morgan DJ, Ryabenkova Y, Bartley JK, Carley AF, Taylor SH, Kiely CJ, Khalid K, Hutchings GJ (2012) Modified zeolite ZSM-5 for the methanol to aromatics reaction. Catal Sci Technol 2:105–112
33. Niziolek AM, Onel O, Floudas CA (2015) Production of benzene, toluene, and xylenes from natural gas via methanol: process synthesis and global optimization. AIChE J 62:1531–1556
34. Wang C, Yang M, Tian P, Xu S, Yang Y, Wang D, Yuan Y, Liu Z (2015) Dual template-directed synthesis of SAPO-34 nanosheet assemblies with improved stability in the methanol to olefins reaction. J Mater Chem A 3:5608–5616
35. Nishiyama N, Kawaguchi M, Hirota Y, Van Vu D, Egashira Y, Ueyama K (2009) Size control of SAPO-34 crystals and their catalyst lifetime in the methanol-to-olefin reaction. Appl Catal A 362:193–199
36. Ren S, Liu G, Wu X, Chen X, Wu M, Zeng G, Liu Z, Sun Y (2017) Enhanced MTO performance over acid treated hierarchical SAPO-34. Chin J Catal 38:123–130
37. Salmasi M, Fatemi S, Najafabadi A (2011) Improvement of light olefins selectivity and catalyst lifetime in MTO reaction; using Ni and Mg-modified SAPO-34 synthesized by combination of two templates. J Ind Eng Chem 17:755–761
38. Tian P, Liu Z, Xu L, Sun C (2001) 05-P-18—Synthesis, characterization and catalysis of SAPO-56 and MAPSO-56 molecular sieves. In: Galarneau A, Fajula F, Di Renzo F, Vedrine J (eds) Studies in surface science and catalysis. Elsevier, Amsterdam, p 248
39. Xu L, Liu Z, Du A, Wei Y, Sun Z (2004) Synthesis, characterization, and MTO performance of MeAPSO-34 molecular sieves. In: Bao X, Xu Y (eds) Studies in surface science and catalysis. Elsevier, Amsterdam, pp 445–450
40. Salih HA, Muraza O, Abussaud B, Al-Shammari TK, Yokoi T (2018) Catalytic enhancement of SAPO-34 for Methanol conversion to light olefins using in situ metal incorporation. Ind Eng Chem Res 57:6639–6646
41. Rostamizadeh M, Taeb A (2015) Highly selective Me-ZSM-5 catalyst for methanol to propylene (MTP). J Ind Eng Chem 27:297–306
42. McIntosh RJ, Seddon D (1983) The properties of magnesium and zinc oxide treated zsm-5 catalysts for onversion of methanol into olefin-rich products. Appl Catal 6:307–314
43. Sanderson RT (1988) Principles of electronegativity. Part I. General nature. J Chem Educ 65:112
44. Tanaka K-I, Ozaki A (1967) Acid-base properties and catalytic activity of solid surfaces. J Catal 8:1–7
45. Politzer P, Murray JS (2018) Electronegativity—a perspective. J Mol Model 24:214
46. Tamura M, Shimizu K-I, Satsuma A (2012) Comprehensive IR study on acid/base properties of metal oxides. Appl Catal A 433–434:135–145

47. Horiuchi T, Hidaka H, Fukui T, Kubo Y, Horio M, Suzuki K, Mori T (1998) Effect of added basic metal oxides on CO_2 adsorption on alumina at elevated temperatures. Appl Catal A 167:195–202
48. Li X, Han D, Wang H, Liu G, Wang B, Li Z, Wu J (2015) Propene oligomerization to high-quality liquid fuels over Ni/HZSM-5. Fuel 144:9–14
49. Niu X, Gao J, Miao Q, Dong M, Wang G, Fan W, Qin Z, Wang J (2014) Influence of preparation method on the performance of Zn-containing HZSM-5 catalysts in methanol-to-aromatics. Microporous Mesoporous Mater 197:252–261
50. Kung HH (1989) Surface acidity. In: Kung HH (ed) Studies in surface science and catalysis. Elsevier, Amsterdam, pp 72–90
51. Engtrakul C, Mukarakate C, Starace AK, Magrini KA, Rogers AK, Yung MM (2016) Effect of ZSM-5 acidity on aromatic product selectivity during upgrading of pine pyrolysis vapors. Catal Today 269:175–181
52. Van der Borght K, Galvita VV, Marin GB (2015) Ethanol to higher hydrocarbons over Ni, Ga, Fe-modified ZSM-5: Effect of metal content. Appl Catal A 492:117–126
53. Zemann J (1965) Crystal structures, 2nd edition. Vol. 1 by R. W. G. Wyckoff. Acta Crystallogr 18:139–139
54. Bibby DM, Milestone NB, Patterson JE, Aldridge LP (1986) Coke formation in zeolite ZSM-5. J Catal 97:493–502
55. Gao J, Zheng Y, Jehng J-M, Tang Y, Wachs IE, Podkolzin SG (2015) Identification of molybdenum oxide nanostructures on zeolites for natural gas conversion. Science 348:686–690